FRS Study of Diffusional Processes in Block Copolymer/Homopolymer Blends Containing Glassy Spherical Micelles†

Wolfgang Schaertl,‡ Kiyoharu Tsutsumi,‡ Kohtaro Kimishima,‡ and Takeji Hashimoto*,‡,§

Hashimoto Polymer Phasing Project, ERATO, JRDC, Japan, 15 Morimoto-Chyo, Shimogamo Sakyoku, Kyoto 606, Japan, and Department of Polymer Chemistry, Graduate School of Engineering, Kyoto University, Kyoto 606-01, Japan

Received January 4, 1996; Revised Manuscript Received May 1, 1996⊗

ABSTRACT: Forced Rayleigh scattering (FRS) was used to study diffusional processes in block copolymer/homopolymer blend systems forming spherical microdomains. Materials used were an asymmetric polystyrene-*block*-polyisoprene copolymer (M_n = 74 000, 21 wt % polystyrene) labeled with photosensitive dyes (o-nitrostilbene or fluorescein) at the end of polystyrene block chains (b-PS) and two kinds of homopolyisoprene (HPI) (M_n = 23 000, M_n = 90 000). Using the lower molecular weight HPI for blending with the block copolymer, b-PS spheres with coronas of polyisoprene block chains (b-PI) strongly swollen by the matrix HPI are obtained (wet-brush system), whereas the HPI matrix having higher M_n yields much less swollen coronas of b-PI (dry-brush system). The differences between these two systems in structural and dynamical behavior were found by small-angle X-ray scattering and FRS studies, respectively. To exclude chain release from the spherical micelles during the measurements, diffusion has been studied close to the T_g of b-PS microdomains. Unexpectedly, FRS signals differed strongly if measured well below or slightly above the T_g of PS microdomains in both intensity and corresponding diffusional processes.

Introduction

Block copolymer/homopolymer blends are of major technical and scientific relevance due to their interesting structural and dynamical behavior. Therefore, many research groups have reported on investigation of various kinds of systems, showing, for example, lamellar,[1−8] cylindrical,[1,2,8] spherical[2] microdomain structures. However, most of these studies were concerned with structural properties of the system, using mainly small-angle X-ray scattering (SAXS) or transmission electron microscopy (TEM) as exploration techniques, whereas information on diffusional behavior of these complicated systems is still scarcely to be found in literature.

Since dynamical processes in such bulk polymer systems are expected to be very slow, special techniques have to be used for investigation. Here, forced Rayleigh scattering (FRS), a holographic grating diffraction technique developed in the last decade,[9−11] provides a powerful experimental method. Previously, diffusional dynamics in lamellar systems had been studied by a few groups[12−14] using FRS. Diffusion in spherical micellar systems, as formed, for example, in 50/50 wt % blends of asymmetric block copolymer A−B (∼15−20 wt % A) and homopolymer B, provides a very interesting subject. Whereas in lamellar systems long-scale translational diffusion of single chains along the polymer interface still should be possible, in spherical systems, single-chain diffusion of block copolymer chains along the interface of the spherical microdomain will not contribute to the FRS signal decay. Therefore it is worthwhile to investigate whether, and at what time scale, diffusional motion is possible at all in such a system.

Previously, some FRS studies on spherical micellar polymer systems had been reported by Inoue et al.,[15] studying solutions of a polystyrene-*block*-poly(ethylenebutylene)-*block*-polystyrene triblock copolymer (SEBS) in a mixed solvent of tetradecane and dibutyl phthalate. This system forms micelles of polystyrene block chain (b-PS) cores and poly(ethylenebutylene) (PEB) coronas. It should be noted here that in such a triblock system, especially at higher block copolymer concentrations, the micelles may have gellike properties, either by some block copolymer chains bridging two different micelles (Figure 1a) or by connected loops (Figure 1b). However, these possibilities (Figure 1a,b) had not been considered in ref 15, and the results were discussed in terms of nonconnected spherical micelles. The authors found two diffusional processes in the ordered state, where micelles are forming a regular, but more or less distorted, lattice according to SAXS measurements. To explain their findings, the authors suggested as a possibility the existence of a dynamical equilibrium between the lattice and a more disordered, fluidlike arrangement of micelles, correspondingly giving rise to two different diffusional processes. Alternatively, isolated block co-

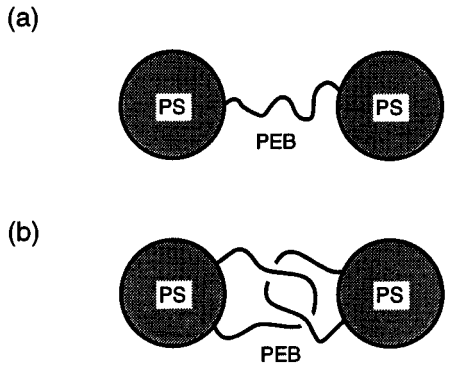

Figure 1. Sketch of formation of gellike cross-linked structures in spherical micelles formed by triblock copolymers, taking as an example the system studied by Inoue et al.,[15] i.e., a polystyrene-*block*-poly(ethylenebutylene)-*block*-polystyrene triblock copolymer in a good solvent for PEB and poor for PS. (a) and (b) show gel formation by bridging and effective cross-linking, respectively.

* Author to whom correspondence should be addressed.
† Presented in part at the American Chemical Society Meeting in Anaheim, April 1995.
‡ Hashimoto Polymer Phasing Project.
§ Kyoto University.
⊗ Abstract published in *Advance ACS Abstracts,* June 15, 1996.

polymer chains might be also present in solution and cause the second faster diffusional mode.[15] Inoue et al. identified their slower diffusional process to be diffusion of spherical micelles as a whole, but they could not provide a definite solution concerning the faster process.[15] These earlier experiments indicate that spherical micellar systems may exhibit quite complex diffusional behavior because the block copolymer, which contains a bleachable photolabel wherefore its diffusion may be probed by FRS, is found in at least three structural modifications, i.e., as part of micelles in the ordered lattice, as part of micelles in the disordered fluidlike state, or as freely diffusing isolated chain.

Whereas Inoue et al. studied systems of micelles in solution, we are interested in the behavior of bulk polymer systems of similar structure, where the solvent is replaced by a homopolymer (i.e., a system of A−B block copolymer containing 15−20 wt % of A block blended with 50 wt % B homopolymer). Note that in both cases the spherical micelles have the same structure of A core with B coronas. Using homopolymer B of far lower molecular weight than the B part of the block copolymer, the micelle coronas B are strongly swollen by this matrix homopolymer (i.e., wet-brush conditions[1,2,16]). On the other hand, using a B homopolymer of comparable or larger molecular weight than the B block chains, the micellar coronas are much less swollen (i.e., dry-brush system[1,16,17]). Recently, Koizumi et al.[18] investigated a spherical micellar system in the wet-brush criterion, a blend of orthonitrostilbene (ONS)-labeled polystyrene-*block*-polyisoprene (SI) with homopolystyrene (HPS) of low molecular weight. Investigations had been carried out at temperatures far above the glass transition of both sphere (composed of polyisoprene block chains (b-PI)) and the matrix (composed of b-PS and HPS). They found that FRS signals $I(t)$ decreased with single-exponential decay, which may give rise to a diffusional mode based on the b-PI sphere as a whole or on release of single block copolymer chains from the micelle and diffusion across the matrix toward joining another micelle (*single-chain jumping process*). Funaki et al.[19] used the same block copolymer as that employed by Koizumi et al. They blended it with HPS having a molecular weight 6 times higher than the HPS employed by Koizumi et al. to study the dry-brush conditions. In this case, very unusual growth decay-type FRS signals had been found, which had been so far attributed to complementary grating effects in the literature.[20−22] The authors' preliminary interpretation was that their unusual signals were based on the specific properties of the ONS label in the sample that had been used.

In this paper we report investigations of the dynamical behavior of fluorescein-labeled polyisoprene-*block*-polystyrene diblock copolymer (IS, labeled at the PS chain end) blended with low and high molecular weight homopolyisoprene (HPI) to obtain wet- and dry-brush conditions, respectively. Systems have been studied at temperatures close to the glass transition of the spheres composed of b-PS in order to restrict the probability of the single-chain jumping process. ONS also had been used as a photolabel during our first experiments, but, depending on bleaching angle and measurement temperature, we sometimes encountered the same strange growth-decay-type signals as reported in ref 19. To avoid these additional complications (possible explanations for this kind of effect will be given in detail in ref 19), we chose to change our photolabel to fluorescein, which had been previously used successfully in FRS studies of diffusion in homopolystyrene systems by Antonietti et al.[23]

Table 1. Characteristics of Polymers Used in These Experiments

specimen	$M_n \times 10^{-4}$	M_w/M_n	w_{PS}
IS	7.4	1.25	0.21
HPI (wet)	2.35	1.36	0
HPI (dry)	9.00	1.10	0

Experimental Section

A. Materials. The IS block copolymer was prepared by a sequential living anionic polymerization technique, polymerization of isoprene first and then styrene. Polymerization was carried out in cyclohexane at 50 °C with *n*-butyllithium as an initiator. The living block copolymer solution was divided into two halves, one being terminated with methanol and the other one with a 50 times excess of α,α′-dichloro-*p*-xylene dissolved in dried and degassed tetrahydrofuran (THF) to introduce a functional chloromethyl group for the labeling reaction at the chain end of the polystyrene block. The large excess amount of α,α′-dichloro-*p*-xylene was used to suppress binarization of the block copolymer chains due to coupling by the bifunctional termination reagent. GPC yielded a binarization rate of less than 5%. It should be noted here that the binarization decreases the effective concentration of labeled block copolymer, although the presence of binarized block copolymer chains (i.e., IS−SI triblock copolymers) should have no significant influence on the microdomain structure and diffusional behavior of our blends (especially so, in the case in which b-PS spheres diffuse as a whole). The functionalized copolymer was reacted with a 10 times excess amount of the cesium salt of fluorescein in a 50/50 wt % mixture of dried THF and *N*,*N*-dimethylformamide (DMF) at 60 °C for 24 h. Usage of a solvent mixture was necessary since the IS copolymer could not be dissolved in the pure DMF usually used for this kind of reaction,[12,13,23] and the solubility of the fluorescein Cs salt was too low in pure THF. Labeled polymers were purified by precipitation of the labeling solution into methanol and frequent washing of the precipitate with cold 50/50 water/methanol mixtures. To be sure to remove excess free fluorescein molecules from the polymer, samples were reprecipitated once from the THF solution into methanol. Uv−visible absorption yielded a labeling efficiency of >60%. Sample characterization by GPC yielded a total molecular weight of $M_n = 7.4 \times 10^4$ ($M_w/M_n = 1.25$), with a PS content of 21 wt %.

As matrix for our wet brush systems, we used a low molecular weight homopolyisoprene (HI) provided by the Kuraray Co., Kurashiki, Japan ($M_n = 23\,500$, $M_w/M_n = 1.36$). The high molecular weight matrix HPI for the dry-brush system was prepared by a living anionic polymerization technique under the same conditions as the preparation of the block copolymer. The sample has been characterized by GPC, giving $M_n = 90\,000$, $M_w/M_n = 1.1$. Table 1 summarizes the characteristics of the polymer specimens used in this paper.

To prepare blends with a spherical microdomain structure, equal amounts of IS block copolymer and HPI were dissolved in THF (5−10% solution); the solution was poured into petri dishes and left standing at room temperature for slow evaporation of the solvent in order to obtain as-cast films. To remove remaining solvent, as-cast films were annealed under vacuum at 100−110 °C for 3 days. We should note here that the label concentration actually proved to be too large for FRS if we were using purely labeled IS (∼1500 monomers/label). To obtain appropriate samples, we had to use a mixture of unlabeled IS with labeled IS at a ratio of 2:1, resulting in a label concentration of ∼5000 monomers/label in the IS/HPI system as recommended in ref 23. Although the samples were stored at room temperature, the photolabel was found to remain photoreactive for more than 5 months. FRS measurements gave reproducible results during this period.

B. Small-Angle X-ray Scattering (SAXS). SAXS measurements were conducted with an apparatus consisting of a rotating-anode X-ray generator (18 kW, MAC-Science Co. Ltd.,

Yokohama, Japan), a graphite monochromator for the incident beam monochromatization, and a one-dimensional position-sensitive proportional counter (PSPC) as a detector. The Cu Kα line with 0.154 nm wavelength was used. The camera length was 1988 mm. All profiles were corrected for absorption of X-ray by sample, air-scattering, and slit-smearing effects as well as thermal diffuse scattering (TDS).

C. Forced Rayleigh Scattering (FRS). Diffusion measurements were performed with a recently constructed FRS setup; technical details have been described previously.[12,13] In principle, the sample is exposed to two coherent interfering light beams originating from an Ar^+ laser operating at a wavelength of 488 nm, power 50−80 mW, for a period of 100−200 ms, to create a diffraction grating by bleaching the photolabel molecules at the positions of the interference maxima within the specimen. The decay in amplitude of this grating, caused by diffusional motion, is probed by detecting the scattering of one of these beams, after attenuation by a factor of 1000 to avoid further bleaching of the sample, at the angle of the first-order Bragg peak. All measurements were carried out in transmission geometry, using bleaching angles θ between 1.5 and 90°.

Samples were prepared by cold pressing at room temperature between two disk-shaped glass plates, forming a specimen of 1 cm diameter and sample thickness from 0.05 to 0.2 mm as adjusted by use of Teflon spacers. In all cases, these samples have been annealed at measurement temperature at least for 2−3 h prior to FRS measurement to let the flow processes relax. At high temperatures, above T = 80 °C, measurements were carried out by shielding specimens under an inert gas atmosphere to suppress thermal oxidation or cross-linking of the b-PI/HPI matrix.

Results and Discussion

A. SAXS Measurements. Figure 2a shows the results of our SAXS measurements for the wet-brush system. The three curves correspond to measurements at a temperature T = 40 °C (curve 1), T = 100 °C after more than 2 h annealing (curve 2), and T = 40 °C after cooling down from 100 °C (curve 3). In all three cases, the same sample had been used and the temperature range corresponds to our FRS measurements discussed later. All of the curves show the typical scattering profiles from spherical microdomains on a cubic lattice, and no significant change in structure is found in the measured temperature range. Figure 2b shows SAXS profiles for a dry-brush system at T = 100 °C (curve 3), and, for comparison, measured data for the wet-brush system (curve 1) as well as data numerically obtained by the paracrystal model[24] (curves 2 and 4, respectively; see further below). It can be clearly seen that the first-order Bragg peak corresponding to the lattice structure of the spherical domains is much less pronounced in the dry-brush system, indicating a more distorted lattice structure than in the wet-brush case.

To analyze the SAXS profiles in a simple way, the cell edge length a (the length of unit cell) in a cubic lattice is determined from the Bragg spacing, d_{hkl}, calculated from the position of the scattering maximum at small q_m which is due to the intersphere interference,

$$d_{hkl} = 2\pi/q_m \tag{1a}$$

$$d_{hkl} = a/(h^2 + k^2 + l^2)^{1/2} \tag{1b}$$

where q_m is the scattering vector of the first-order Bragg peak of intersphere interference, and h,k,l are the Miller indices of the diffraction planes. Note that, due to extinction rules, only certain d_{hkl} are visible in the SAXS data. d_{hkl} and a are interrelated to one another by

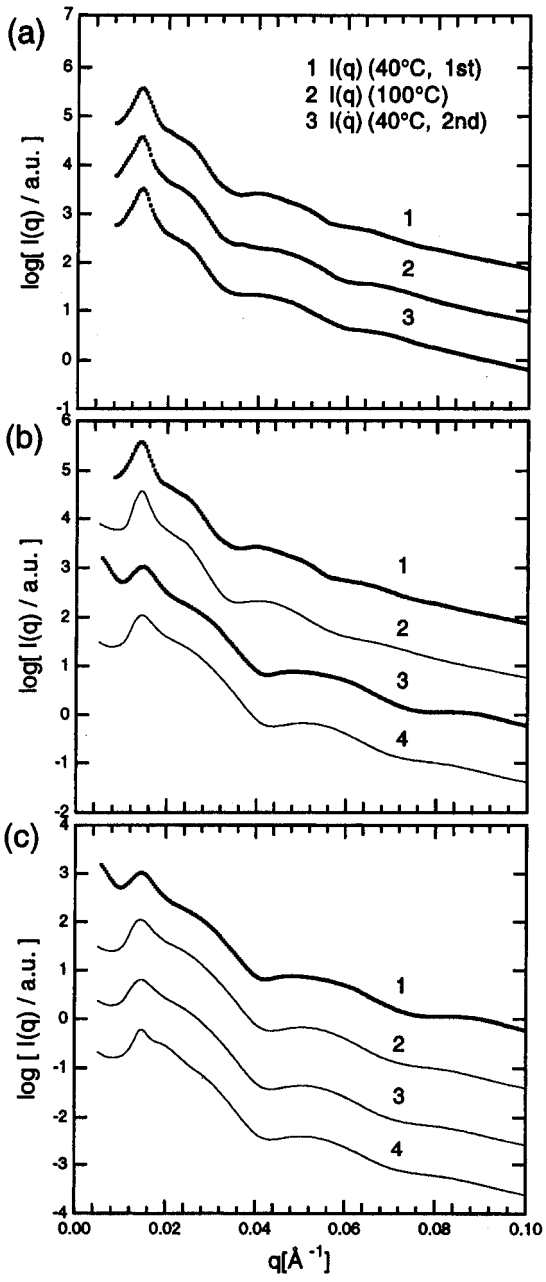

Figure 2. SAXS profiles of SI diblock/HPI homopolymer 50/50 wt % blend for (a) the wet-brush system, showing that structure remains almost unchanged in the temperature interval. (b) shows the comparison of the SAXS profiles between the wet- and dry-brush system as well as numerically obtained scattering curves using paracrystal model. (c) shows the comparison of the SAXS profile for the dry-brush system with numerically obtained fitting curves, assuming various lattice types.

$$a_{SC} = d_{100} \tag{2a}$$

$$a_{FCC} = 3^{1/2} d_{111} \tag{2b}$$

$$a_{BCC} = 2^{1/2} d_{110} \tag{2c}$$

for simple cubic (SC), face-centered cubic (FCC) or body-centered cubic (BCC) lattice, respectively.

The SAXS profiles also show a broad maximum at larger q due to intraparticle interference of the single spherical domains. From the peak position, q_R, the average sphere radius R is calculated according to

Table 2. Characteristic Parameters and Assumed Lattice Type To Obtain Numerically Calculated SAXS Profiles Shown in Figure 3b and Figure 3c

sample	$\Phi_{PS,A}$	lattice type	R (nm)	ΔR (nm)	a (nm)	$\Delta a/a$	$\Phi_{PS,SAXS}$
wet brush	0.089	BCC	14.0	1.5	60.5	0.15	0.104
dry brush	0.090	BCC	11.3	2.0	58.0	0.20	0.062
		FCC	11.3	2.0	71.0	0.28	0.068
		SC	11.3	2.0	43.0	0.18	0.076

$$R = 5.765/q_R \quad (3)$$

Using R and a, the volume fraction of PS cores can be calculated for the various lattice types and compared to $\phi_{PS,A}$, the analytical volume fraction of PS cores determined from the sample composition.[2]

More accurate results than those determined from simply taking the peak positions of the scattering profiles may be obtained using so-called paracrystalline fitting models.[24] The paracrystal analysis provides the cell edge length a, mean radius of sphere R, a standard deviation in the probability distribution of the sphere radius ΔR, and the paracrystal lattice distortion factor $\Delta a/a$. The best results of the fitting procedure are presented in Figure 2b, where curves 1 and 3 are the experimental data of the wet- and dry-brush systems, respectively, and curves 2 (wet-brush) and 4 (dry-brush) are the calculated fits. Both curves were obtained by assuming a BCC-type lattice. The mean radius of spheres R for the wet-brush system is larger than that of the dry-brush system, whereas the dry-brush system fit has a larger lattice distortion parameter ($\Delta a/a$), indicating a more distorted lattice structure as already mentioned above. Figure 2c shows the comparison of best-fit profiles based on various lattice types, BCC (curve 2), FCC (curve 3), and SC (curve 4) for the dry-brush system (curve 1). The parameters used for calculating the fits given in Figure 2b and c are summarized in Table 2.

The analytical volume fraction of the b-PS cores ($\Phi_{PS,A}$) has been calculated using the composition of the blend (~50 wt % SI) and the block copolymer composition (SI, 21 wt % b-PS) on the basis of a complete segregation of b-PS from b-PI and HPI. Densities used were 1.053 g/cm^3 for b-PS and 0.913 g/cm^3 for b-PI and HPI. This volume fraction is compared with the result from the fit to our experimental SAXS data, $\Phi_{PS,SAXS}$ for the wet-brush system, the two volume fractions given in Table 2 are comparable, and the assumption of the BCC lattice is most appropriate. For the dry-brush system, the fitting curves with FCC or BCC assumption look more appropriate than SC, whereas comparison of the volume fractions favors a SC-type structure. Note here that the paracrystalline distortion factor for the dry-brush system is very large, which was not considered in calculating $\Phi_{PS,SAXS}$ where only mean radius R and mean cell edge length a had been used. Taking into account all of the above, we believe the structure of the dry-brush sample also to be BCC as reported in literature.

We note here that dry-brush micelles are usually expected to have larger radii than corresponding wet-brush systems: the dry brush is less swollen, wherefore a smaller curvature of the sphere is expected. However, kinetic effects during the solvent casting process as well as the much larger viscosity of the dry-brush matrix may have pinned the growth of the micelles in our dry-brush system at smaller sphere radii than the corresponding wet-brush system during the solvent evaporation process.

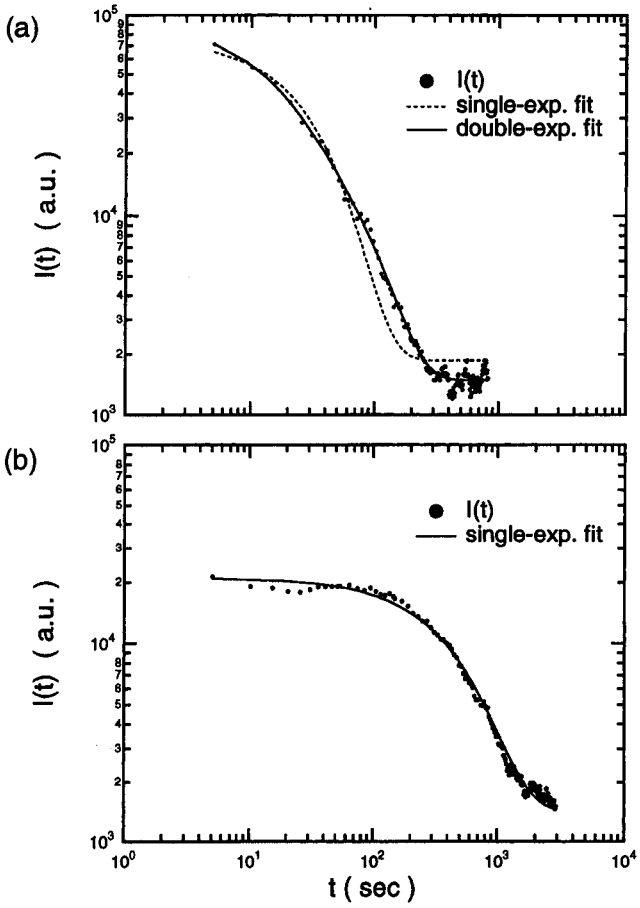

Figure 3. Typical FRS profile for (a) the wet-brush system measured at $T = 100$ °C with bleaching angle $\theta = 38°$ and for (b) the dry-brush system measured at $T = 120$ °C with bleaching angle $\theta = 42.5°$. Symbols correspond to measured data. Solid and dashed lines are fitting curves based on eq 4. For the wet-brush system a double-exponential fit is preferable, while for dry-brush system, a single-exponential fit has good agreement with measured data.

Finally, knowing both the average volume of a single spherical domain and the composition of a single block copolymer chain, it is possible to determine the average number of block copolymer chains per sphere, N_{SP}. This simple calculation, taking into account the bulk density of b-PS as 1.053 g/mL, yielded a value of $N_{SP} \approx 320$ for dry brush and 400 for wet brush.

B. FRS Measurements. (i) FRS Signals. A typical decay of the FRS intensity could be presented with the single- or double-exponential fitting functions according to eq 4:

$$I(t) = [A \exp(-t/\tau_1)]^2 + C \quad (4a)$$

$$I(t) = [A_1 \exp(-t/\tau_1) + A_2 \exp(-t/\tau_2)]^2 + C \quad (4b)$$

In these equations, A, A_1, and A_2 denote amplitudes and τ_1 and τ_2 are relaxation times of the signal decay, while C is a constant background value contributing incoherently to the signal and therefore identical to the FRS intensity measured before bleaching.[9-13] Although sometimes a coherent scattering background B has to be considered in eq 4,[9-13] this was not necessary in our case, where B was found to be negligible by measuring the FRS intensity before bleaching and after decay of the signal.

Figure 3a shows a typical FRS signal of our wet-brush system at $T = 100$ °C, FRS bleaching angle $\theta = 38°$,

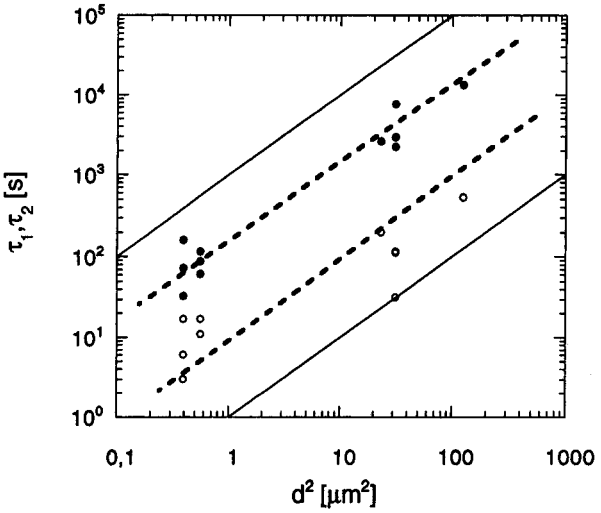

Figure 4. Relaxation times τ_1 and τ_2 resulting from fitting the FRS intensities $I(t)$ according to eq 4b, plotted vs the square of the lattice spacing d in double-logarithmic scale. Solid lines indicate slope 1 in the figure, which is expected for diffusive processes; dashed lines show least-squares fits of the two processes. Data were obtained from a wet-brush system at $T = 100$ °C.

Table 3. Parameters Used for Fitting the Decay in FRS Intensity with Single- and Double-Exponential Functions

sample		A_1	τ_1 (s)	A_2	τ_2 (s)	C
wet brush	single-exp fit	273.5	58.91			1852
	double-exp fit	132.5	17.33	171.8	116.1	1474
dry brush	single-exp fit	140.4	910.5			1416

with single- and double-exponential fitting curves. It is obvious that the data cannot be described by the single-exponential decay function, whereas the double-exponential fit shows excellent agreement. It also should be noted that the uncertainties of the parameters obtained from the double-exponential fit are the order of only 3−5%. We conclude at this stage that in the wet-brush system at least two different dynamical processes with comparable amplitude are present.

In Figure 3b, a typical FRS signal measured from a dry-brush system at $T = 120$ °C, $\theta = 42.5°$ is given together with the single-exponential fit, which, opposite to the wet-brush system, describes the data quite well. Therefore, we may assume that the FRS decay is dominated by a single dynamical process, although diffusional processes on different time scales with much smaller amplitude may still be present outside the time window of our experiment. Fitting parameters used here are summarized in Table 3.

(ii) Analysis of *d* Dependence of Relaxation Rates. To assure the diffusive character of the signal decay, one has to measure $I(t)$ at different bleaching angles, and, correspondingly, holographic lattice spacings d.[13,15] Plotting the relaxation times τ vs d^2 in double-logarithmic scale, Fickian diffusion, for example, should reveal itself by a straight line with slope 1 according to

$$\log \tau = -\log(4\pi^2 D) + \log d^2 \qquad (5)$$

where D is the diffusion coefficient.[9,11]

Figure 4 shows our results for the wet-brush sample, measured at a variety of bleaching angles at $T = 100$ °C. All FRS signals had been fitted by double-exponential decays. The filled circles in Figure 4 correspond to the slower, and the open circles to the faster, of the two processes. We also indicated the slope of unity, predicted by eq 5, by two solid lines. Although the data show comparably large scatter even at identical d^2, both processes can be clearly distinguished and fulfill quite nicely the assumption of Fickian diffusion according to eq 5. The broken lines show least-squares fit of the two processes. We therefore may conclude that our wet-brush system definitely shows two diffusive processes, which differ by about one decade in D. Here, it should be noted that the uncertainty of the relaxation times for each of these processes is the order of roughly a half decade. However, as clearly can be seen in Figure 4, no overlap of time scales is found in the case of the two processes, as had been seen previously by Ehlich et al.[13] Therefore, opposite to the statement given in ref 13, we understand our results not in terms of a broad distribution in relaxation time of a single dynamical process but as the presence of two distinctly different diffusional modes, each of which may have some uncertainty in relaxation time due to a nonuniform structure within the specimen.[13]

A detailed discussion about the origin of scatter of relaxation times determined from FRS measurements at different positions within a specimen of lamellar microdomain structure is given in ref 13. We will not repeat this discussion here, since most of the arguments may apply also to our case, and so far no better explanations have been found besides the existence of structural differences as for example, in our case, local fluctuations in orientation of the cubic lattice, the paracrystalline distortions, and at grain boundaries within the sample. The existence of two distinct processes in our case is in good agreement with the previous findings of Inoue et al.[15]

(iii) Temperature Dependence of FRS Signal Intensity. The reader may have noted that, although we originally had intended to study spherical micelles with PS cores far below the T_g of PS to avoid any contribution of the single-chain jumping process to the FRS signal,[18,19] results presented so far had been measured very close to or even slightly above the T_g of b-PS. This is mainly due to the fact that we encountered a very strange and unexpected, but extremely interesting phenomenon during our FRS experiments below T_g. In Figure 5a, we show FRS decays measured for the same wet-brush sample under identical conditions (bleaching angle $\theta = 37°$, power 75 mW, bleaching time 300 ms, sample thickness 0.2 mm) as in Figure 3 except for measurement temperature (curve 1, $T = 80$ °C, curve 2, $T = 50$ °C). There is a dramatic increase in signal intensity at the higher temperature, which seems to correspond to a more effective bleaching process and therefore more pronounced holographic grating in this case. Also, the decay process seems to be slower at higher temperature, which may possibly be explained as follows: the diffusional process dominating the decay at $T = 80$ °C is not identical to the process dominating the decay at $T = 50$ °C!

Even more evidence of this unusual effect is shown in Figure 5b, where the FRS intensity I_0 right after the bleaching relative to the intensity C in eq 4 is plotted as a function of $1/T$. We investigated the relative signal intensities I_0/C of many measurements at nearly identical bleaching angles ($\theta \sim 40°$) as a function of $1/T$. It can be clearly seen that, in all cases, even for different samples such as wet brush (filled circles, data numbered 1) and dry brush (open circles, data numbered 2) with fluorescein label or wet brush with ONS photolabel

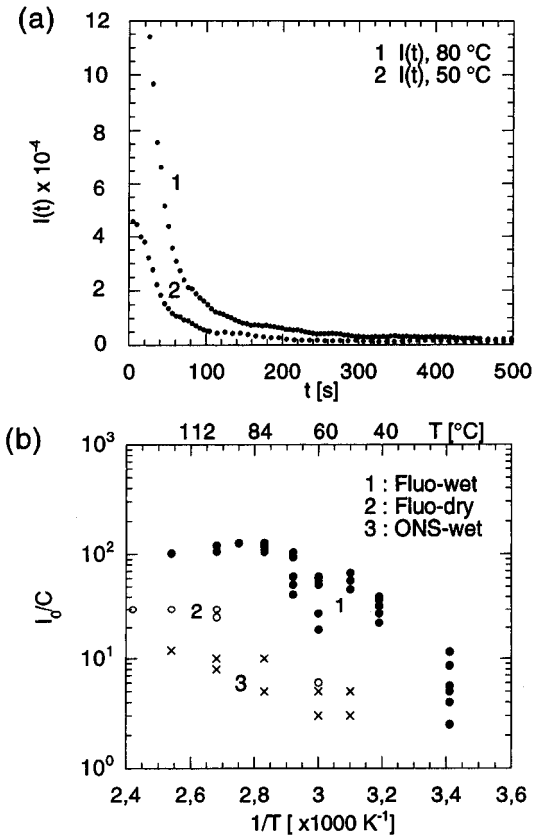

Figure 5. (a) FRS signals for the wet-brush system measured at $T = 80$ °C (curve 1) and $T = 50$ °C (curve 2) with bleaching angle $\theta = 37°$. Note the large difference in intensity, as well as the fact that at higher temperature the signal seems to decay slower. (b) Normalized FRS intensity I_0/C (C, background scattering before bleaching; I_0, FRS intensity immediately (5 s) after bleaching) as a function of $1/T$ for both fluorescein-labeled (filled circles, wet brush; open circles, dry brush) and ONS-labeled (crosses, wet brush) samples.

(crosses, data numbered 3), there is a large increase in FRS intensity with increasing temperature. Above $T \approx 70$ °C, corresponding to $1/T = 0.0029$ K^{-1}, the signal intensities do not significantly increase any further. Note here that the difference in signal intensities of fluorescein labeled wet- and dry-brush systems at high temperatures (curves 1 and 2, respectively) are due to a difference in label concentration of the specimen, respectively. Since the only characteristic temperature of our system close to the transition regime shown in Figure 5b is the T_g of b-PS, supposed to be approximately $T_g = 80-90$ °C for our PS block of $M_n = 16\,000$, and the phenomenon is found for different photolabels and matrix polymers, it is very tempting to attribute our findings to the glassy state of the b-PS core, in which the photolabel is imbedded. We would like to note here that an effect of the glassy state of the matrix on the photoreaction also had been found previously by Antonietti et al.,[25] who explained their findings as follows: during the FRS bleaching process, the photoproduct is formed from an excited state with a very short lifetime, typically the order of $10^{-6}-10^{-10}$ s. During this short time interval, the molecular transformation into the photoproduct has to take place. In the case of a glassy state of the matrix, it therefore seems plausible that not enough free volume can be generated in such a short time, and the photoreaction is strongly inhibited.[25]

(iv) Interpretation of Differences in FRS Signals at High and Low Temperatures for Both Wet- and Dry-Brush Systems. In the case of wet-brush systems, the existence of a fast process at low temperatures far below the T_g of b-PS, although with much smaller amplitude than any signal at higher T, seems to indicate that some of the block copolymer chains are more mobile than the b-PS blocks of the b-PS micellar core. We speculate this species to be isolated block copolymer chains that are not part of a micellar domain. Further, the extremely low signal intensity for dry-brush systems at low temperatures should be noted in Figure 5b, in the context of our speculations, corresponding to an extremely small amount of isolated block copolymer chains. This may be understood in terms of the critical micelle concentration (cmc) of the dry-brush system being much smaller than for the wet-brush case, corresponding to the dry-brush HPI being a less suitable solvent for the SI block copolymer chains compared to the wet-brush HPI.

(v) Discussion of Dynamical Processes in Wet- and Dry-Brush Systems. Since the temperature range covered was below 120 °C for all experiments in this paper, we expect the PS core of the spherical domains to be too viscous to allow for either chains being released from the domains or free block copolymer chains joining the domains. This is underlined by our results from SAXS (Figure 2a), where no change in domain radius is found between $T = 40$ and 100 °C. We may therefore conclude that the two distinct processes found at $T = 100$ °C are caused by translational diffusion of spherical domains as a whole and free block copolymer chains, respectively. We find it difficult to imagine spherical domains diffusing in the well-ordered lattice state. We nevertheless agree that, as somehow indicated also by the lattice distortion and experimental findings in colloidal systems,[26] the lattice structure may be not permanent but in dynamical equilibrium with a more disordered, fluidlike arrangement of micelles, where translational diffusion of spheres as a whole is more probable. If this is the case, so far still speculative, fluctuation between fluid and crystalline states is comparably fast, only the translational diffusion of spherical micelles in the fluidlike state should contribute to the FRS decay. Consequently, the FRS signal will always decay to the background intensity level C identical to the intensity before bleaching. On the other hand, the existence of a more permanent lattice with highly immobile spherical micelles should result in the FRS signal decaying toward a background $B + C$ significantly larger than the incoherent background C before bleaching, because the holographic lattice is partly maintained within the immobile crystalline parts of the sample.

The existence of two dynamical processes based on diffusion of single chains and diffusion of spheres as a whole in the fluidlike state may also be deduced from Figure 6 given in ref 15, where no discontinuity in diffusion in crossing the phase boundary from fluidlike to crystalline arrangement of micelles (which had been determined by the appearance of higher order peaks in the SAXS pattern[15]) could be seen. The faster of the two processes found below the order−disorder transition (ODT) of the system just seems to be the extrapolation of the diffusional process of isolated block copolymer chains measured above ODT.[15]

(vi) Semiquantitative Analysis of Diffusion Coefficients in Terms of the Stokes−Einstein Relation. In Figure 6a we present the self-diffusion coefficients determined according to

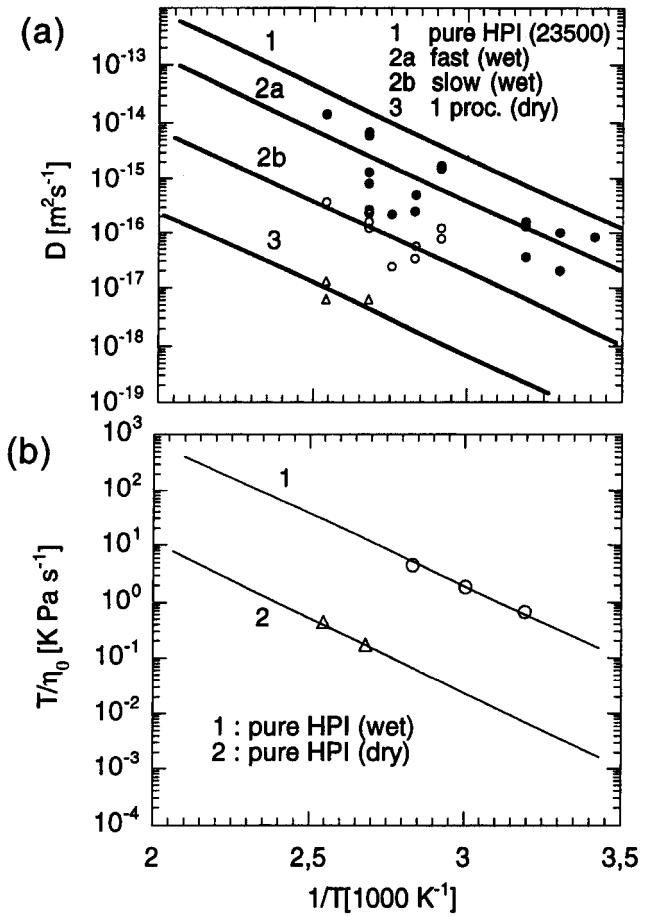

Figure 6. (a) Self-diffusion coefficients D as a functcion of $1/T$ for both wet-brush (circles) and dry-brush (triangles) systems. Solid line 1 corresponds to self-diffusion of ONS-labeled pure polyisoprene (HPI) of comparable molecular weight as wet-brush HPI, taken from the literature.[13] (b) T/η_0 as a function of $1/T$ for both neat homopolyisoprenes used in the wet-brush (circles) and dry-brush (triangles) blends. The slopes in the (a) and (b) are almost identical.

$$D = d^2/(4\pi^2\tau) \tag{6}$$

for both wet- and dry-brush systems as a function of $1/T$. For comparison, also the diffusivity of pure HPI corresponding to the wet-brush matrix has been taken from the literature[13] and plotted as a straight line (line 1). Although the data show comparably large scatter, the two diffusional processes of the wet-brush system are well separated by about one decade (see symbols with filled and unfilled circles, lines 2a and 2b, respectively). Also the fact that the fast process (filled circles) is about one decade slower than the diffusion of pure HPI (HPI wet) seems to agree well with the fact of the block copolymer molecular weight M being ~3 times larger than that of HPI wet. This dependence of D on M corresponds very well to the results of Antonietti et al.,[23] who have studied self-diffusion of PS tracer chains of various molecular weights in a given PS matrix by FRS. Concerning the dry brush, so far only a single process had been found (line 3). This process seems to be slower than the slow process of the wet-brush system by a little bit more than one decade.

For a given system composed of given matrix and diffusant, the self-diffusion coefficient D is related to the zero shear viscosity of the matrix η_0 by the Stokes–Einstein relation given by eq 7.

$$D = kT/(6\pi\eta_0 R_H) \tag{7a}$$

$$\log D = \log(T/\eta_0) + C \tag{7b}$$

where k is the Boltzmann constant and R_H the effective Stokes radius of the diffusant, which is only a weak function of T. Equation 7b is obtained by factoring eq 7a by the constant C, which depends only on the size of the diffusant. If eq 7 is valid in our bulk polymer system, when log D or log (T/η_0) is plotted vs $1/T$, both curves should show identical slopes, because in our case R_H is effectively independent of T from SAXS experiments as a function of T.

On the basis of the discussion above, we have measured the zero shear viscosities of neat HPI forming wet and dry brush using a rheometer (Rheometrics mechanical spectrometer Model RMS800). T/η_0 are plotted as a function of $1/T$ in Figure 6b, and we could obtain almost identical slope in both Figure 6a and b.

Whereas this assumption seems to be perfectly fulfilled by all our data within experimental accuracy, i.e., all data sets have identical slopes, one should be careful in calculating a hydrodynamic radius R_H from the diffusion coefficients D and matrix viscosities η_0 in our case. The Stokes–Einstein diffusional model assumes a nonstructured homogeneous matrix, which is not at all to be expected in the case of bulk block copolymer systems. However, from our diffusion coefficients we get an effective hydrodynamic radius of $R_H \approx 70$ nm for the wet-brush (considering only the slower D of the two diffusional processes!) and $R_H \approx 20$ nm for the dry-brush case. Note that the ratio of ~3.5 is much larger than the ratio of the core radii R given in Table 2. Whereas we should not attribute too much physical meaning to the absolute values according to the reason stated above, the results indicate a qualitative difference of wet- and dry-brush micelles: the dry-brush micelles (smaller Stokes radius) diffuse significantly faster than expected from the difference in matrix viscosities of wet- and dry-brush HPI. This effect may be explained by the following two physical factors: (i) the wet-brush micelles are heavily swollen by the matrix polymer, wherefore the effective sphere radius is expected to be much larger than in the dry-brush case; (ii) the wet-brush micelles are in a more ordered lattice, wherefore their translational diffusion should overcome a larger energy barrier associated with conformational changes in the coronar chains. This model is supported by our SAXS results, where at nearly identical analytical volume fractions the dry-brush lattice was found to be far more distorted than in the wet-brush system as judged from the data $\Delta a/a$ in Table 2. This may prove that in the wet-brush system coronal chains tend to be stretched out into the matrix phase and their interactions are less screened by the intervening matrix homopolymer chains. In addition, theoretical considerations of Leibler and Pincus[27] also suggest that wet-brush micelles have much larger effective radii than dry brushes, leading to more ordered structures and comparatively slower self-diffusion of spherical micelles as a whole.

(vii) Summary of Scenario in Wet- and Dry-Brush Spherical Micellar Systems. Figure 7 sketches our understanding of the scenario that is valid both for wet- and dry-brush systems, mainly based on the experimental finding of an increase of signal intensity with increasing temperature. Only block copolymer chains are sketched, found both as single chains (free block chain, FB) and as part of spherical micelles

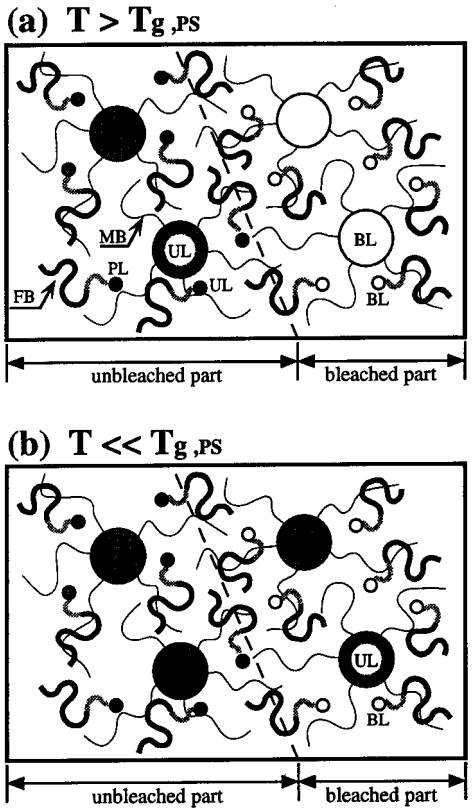

Figure 7. Influence of temperature on signal intensity. Small circles, photolabel (PL) bleached (BL; open circles) and unbleached (UL; filled circles); large circles, b-PS core containing mainly unbleached (UL; dark cores) or bleached (BL; unfilled cores) labels. (a) Bleaching of photolabels of both free single block copolymer chains (FB) and micellar cores at high temperatures; (b) inhibition of bleaching of photolabels within glassy micellar cores at low temperatures.

(micellar block chain, MB). Small circles at one end of the single chains indicate the photolabel (PL). The bleached state (BL) of the label corresponds to open circles or unfilled micellar cores, respectively. On the other hand, unbleached labels are shown by filled circles in the case of isolated chains FB or dark micellar cores (UL). Whereas at high temperatures both kinds of labeled species are bleached (Figure 7a), at low temperatures (Figure 7b) bleaching within the glassy core region is expected to be strongly inhibited. Correspondingly, this leads to an increase in FRS signal intensity with temperature.

Figure 8 schematically shows the differences of wet- and dry-brush systems, based on the experimental findings: (i) the relative intensity decrease with lowering temperature is more pronounced in the dry-brush case; (ii) dry-brush FRS measurements gave single-exponential decaying FRS signals at high temperatures (but nearly zero signal at low temperatures). The figure indicates the difference in amount of isolated block copolymer chains in the wet- (Figure 8a, a larger amount) and dry-brush case (Figure 8b, a smaller amount), which consequently results in the experimental findings mentioned. We may interpret our findings, as mentioned above, in terms of a difference in cmc for wet- and dry-brush systems, i.e., cmc (dry brush) < cmc (wet brush).

Figure 9a sketches the ordered lattice state, where diffusion of spherical micelles as a whole should be strongly inhibited in our opinion, as stated above. The crystalline state has been supposed to be in dynamical equilibrium with a less ordered fluidlike arrangement

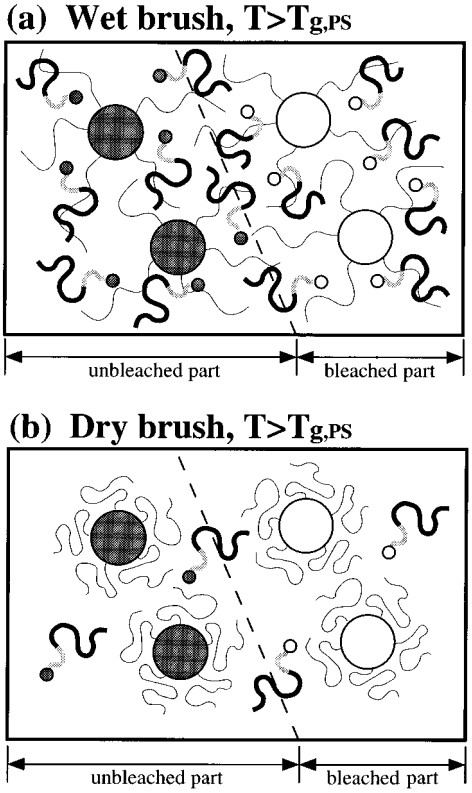

Figure 8. Sketch of the difference in amount of isolated block copolymer chains (FB) in the wet-brush (a) and dry-brush system (b). Shown is the state after bleaching at high temperatures (cf. Figure 7).

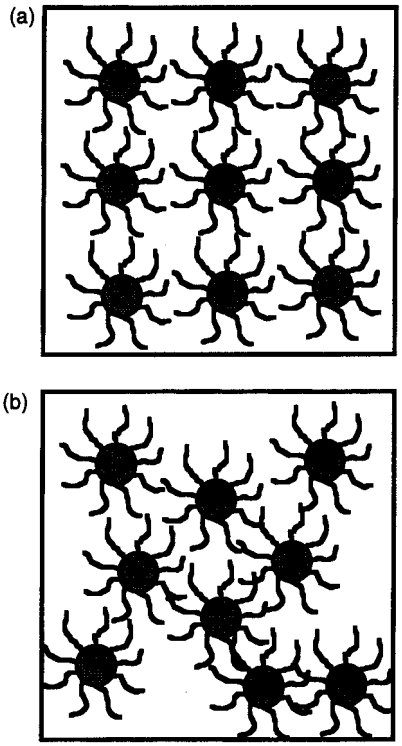

Figure 9. Scenario of diffusion of spherical micelles: (a) spherical micelles in the ordered lattice state, no diffusion; (b) spherical micelles in the disordered state, diffusion; (in both cases, only the block copolymer is sketched; the reader is supposed to imagine all of these diffusants being imbedded in a matrix of HPI).

of micelles as sketched in Figure 9b. We believe that diffusion of the sphere as a whole should mainly take place in this fluidlike region, but crystalline regions

always change rapidly into fluidlike and vice versa, wherefore the FRS grating is never found to be partly permanent, and correspondingly, the FRS signals always decay to the same background as prior to bleaching. Note here that the fraction of the fluidlike regions is greater in the dry-brush micelles than in the wet-brush micelles, as revealed from the paracrystal analysis of the SAXS results. Therefore, mobility of the dry-brush spherical micelles should be comparatively faster, corresponding to a smaller hydrodynamic radius as discussed in (vi).

Summary

We have presented SAXS and FRS studies of a IS/HPI polymer blend forming spherical micelles with b-PS cores in a matrix of b-PI and HPI. Using matrix HPI of two different molecular weights, both wet- and dry-brush conditions have been investigated. From both structural and dynamical properties, the dry-brush system seems to have a smaller effective hydrodynamic radius of the spherical micelle, which is plausible taking into account the smaller degree of swelling of the b-PI coronas by the matrix homopolymer. In the wet-brush system, two diffusional processes have been found in the FRS signals and attributed to diffusion of the spherical micelle as a whole (as a slower process) and free block copolymer chains (as a faster process), respectively. The fact that the dry-brush samples showed mainly single-exponentially decaying FRS signals had been explained by a smaller amount of free block copolymer chains in these samples: the FRS signal decays only through diffusion of the micelle as a whole.

Unexpectedly, a strong dependence of FRS intensity on measurement temperature had been found, which was explained by inhibition of the photoreaction in the glassy matrix of the b-PS micellar cores. This assumption also gave plausible agreement with the scenario of free block copolymer chains diffusing in the HPI matrix, since the photolabels of these chains should be located in a less solid environment than the labels within the micellar cores. Therefore, at temperatures well below the T_g of b-PS, the FRS signals decay mainly by single-chain diffusion while the b-PS cores remain nearly untouched by the bleaching process and hence invisible. At higher temperatures, the labels within the cores are also bleached, and diffusion of the spherical micelles as a whole becomes the dominating part of the FRS signals.

Acknowledgment. We are grateful to Dr. T. Ohnaga for supplying the low molecular weight HPI, and to Mr. K. Matsuzaka for help with the dynamical−mechanical measurements. We also thank Prof. Dr. M. Antonietti for helpful discussions.

References and Notes

(1) Hashimoto, T.; Tanaka, H.; Hasegawa, H. *Macromolecules* **1990**, *23*, 4378.
(2) Tanaka, H.; Hasegawa, H.; Hashimoto, T. *Macromolecules* **1991**, *24*, 240.
(3) Winey, K. I.; Thomas, E. L.; Fetters, L. J. *Macromolecules* **1991**, *24*, 6182.
(4) Banaszak, M.; Whitmore, M. D. *Macromolecules* **1992**, *25*, 2757.
(5) Hong, K. M.; Noolandi, J. *Macromolecules* **1983**, *16*, 1083.
(6) Whitmore, M. D.; Noolandi, J. *Macromolecules* **1985**, *18*, 2486.
(7) Tanaka, H.; Hasegawa, H.; Hashimoto, T. *J. Appl. Cryst.* **1991**, *24*, 672.
(8) Tanaka, H.; Hashimoto, T. *Macromolecules* **1991**, *24*, 5713.
(9) Eichler, H. J.; Salje, G.; Stahl, H. *J. Appl. Phys.* **1973**, *4*, 5383.
(10) Eichler, H. J.; Guenther, P.; Pohl, D. W. In *Laser-Induced Dynamic Gratings*; Springer Verlag: Berlin, 1986.
(11) Kogelnik, H. *Bell. Syst. Tech. J.* **1969**, *48*, 2909.
(12) Ehlich, D.; Takenaka, M.; Okamoto, S.; Hashimoto, T. *Macromolecules* **1993**, *26*, 492.
(13) Ehlich, D.; Takenaka, M.; Hashimoto, T. *Macromolecules* **1993**, *26*, 492.
(14) Eastman, C. E.; Lodge, T. *Macromolecules* **1994**, *27*, 5591.
(15) Inoue, T.; Nemoto, N.; Kurata, M. *Bull. Inst. Chem. Res. Kyoto Univ.* **1988**, *66* (3), 194.
(16) Koizumi, S.; Hasegawa, H.; Hashimoto, T. *Makromol. Chem., Macromol. Symp.* **1992**, *62*, 75.
(17) Koizumi, S.; Hasegawa, H.; Hashimoto, T. *Macromolecules* **1994**, *27*, 6532.
(18) Koizumi, S. Ph.D. Thesis, Kyoto University, Kyoto, Japan, 1995.
(19) Funaki, K.; Schaertl, W.; Hashimoto, T.; Sillescu, H., in preparation.
(20) Rhee, K. W.; Gabriel, D. A.; Johnson, C. S., Jr. *J. Phys. Chem.* **1984**, *88*, 4010.
(21) Park, S.; Yu, H.; Chang, T. *Macromolecules* **1993**, *26*, 3086.
(22) Sung, J.; Chang, T.; Lee, J. W.; Pak, H. *Bull. Korean Chem. Soc.* **1993**, *14* (1), 4.
(23) Antonietti, M.; Coutandin, J.; Gruetter, R.; Sillescu, H. *Macromolecules* **1984**, *17*, 798.
(24) Matsuoka, H.; Tanaka, H.; Hashimoto, T.; Ise, N. *Phys. Rev. B* **1987**, *36*, 1754. Matsuoka, H.; Tanaka, H.; Iizuka, N.; Hashimoto, T.; Ise, N. *Phys. Rev. B* **1990**, *41*, 3854.
(25) Antonietti, M., private communication.
(26) Ito, K.; Nakamura, H.; Yoshida, H.; Ise, N. *J. Am. Chem. Soc.* **1988**, *110*, 6955.
(27) Leibler, L.; Pincus, P. A. *Macromolecules* **1984**, *17*, 2922.

MA9600116